for the RR spectral shifts upon HbCO photolysis.

Very recently Rothberg et al.[17] have obtained picosecond infrared spectra on photolyzed HbCO that indicate a transient high-yield photoproduct with a 2-ps lifetime and a CO stretching frequency suggestive of a high-spin heme adduct. The persistence of such a complex for times longer than the electronic relaxation to the high-spin state has previously been considered[18] as an explanation for the heme core size expansion which is detected in RR transient spectra extending to 10 ns. This explanation was rejected for the longer time scale, but a 2-ps lifetime for a high-spin Fe–CO complex as suggested by the results of Rothberg et al. is not implausible. Although ν_4 is only weakly dependent on the porphyrin core size,[8] the proposed CO binding to the high-spin heme might contribute to the early ν_4 shift through polarization effects. Indeed it is possible that there are multiple contributions to the ν_4 shift on the ~2-ps time scale, from heating, from partially unrelaxed electronic states, and from undissociated CO. The heating effect itself needs to be evaluated in an experimental system which is more closely related to the HbCO photoproduct than is the ν_{10} band of NiOEP.

(17) Rothberg, L.; Jedju, T. M.; Austin, R. H., submitted for publication.
(18) Dasgupta, S.; Spiro, T. G. *Biochemistry* **1986**, *25*, 5941–5948.
(19) Czernuszewicz, R. S. *Appl. Spectrosc.* **1986**, *40*, 571–573.
(20) Alden, R. G.; Crawford, B. A.; Ondrias, M. R.; Shelnutt, J. A. *Proc. Int. Conf. Raman Spectrosc., XI*; Clark, R. J. H., Long, D. A., Eds.; Wiley: New York, 1988; p 541.

Conclusions

NiOEP is clearly ruffled in solution, as evidenced by activation of several of the out-of-plane modes seen in tetragonal crystals.

In-plane skeletal mode frequencies of NiOEP in solution are intermediate between tetragonal and triclinic crystal frequencies, suggesting an intermediate structure.

A large ν_{10} band width implies a range of structures in solution.

These observations, as well as the temperature dependence of the ν_{10} frequency, are suggested to result from anharmonic potentials, possibly double-welled, for the γ_{12} and γ_{14} pyrrole swiveling modes, which arise from the countervaling forces favoring planar versus ruffled NiOEP.

This special effect does not apply to metalloporphyrin bands in general, and the NiOEP ν_{10} temperature dependence is not a reliable guide to the magnitude of heating effects expected in pulsed laser experiments on heme proteins.

Acknowledgment. This work was supported by NIH Grant GM33576. We are deeply grateful to Dr. J. R. Kincaid, Marquette University, for providing us with samples of NiOEP isotopomers and to Drs. R. H. Austin and L. Rothberg for communicating results of their work prior to publication.

Registry No. NiOEP, 24803-99-4.

Characterization of the Electronic Structure of 4′,6-Diamidino-2-phenylindole

Mikael Kubista,* Björn Åkerman, and Bo Albinsson

Contribution from the Department of Physical Chemistry, Chalmers University of Technology, 412 96 Gothenburg, Sweden. *Received December 16, 1988*

Abstract: We characterize the electronic structure of 4′,6-diamidino-2-phenylindole (DAPI) in terms of electronic transition energies, transition moment directions, and oscillator strengths in the UV–vis region. The study is based on linear dichroism and fluorescence anisotropy measurements of DAPI dissolved in poly(vinyl alcohol) film, magnetic circular dichroism in aqueous solution, and circular dichroism on DAPI dissolved in *d*-tartrate and bound to DNA.

The cation 4′,6-diamidino-2-phenylindole (DAPI) binds to double-stranded DNA with a concomitant increase in fluorescence quantum yield.[1] This property has made DAPI very useful as a probe for DNA in gel electrophoresis,[2,3] in DNA protein interactions,[4–6] in cytochemical investigation,[7–12] and for staining of mammalian chromosomes.[13] The binding of DAPI to DNA is reversible, and the molecule binds in two spectroscopically distinct sites, both located in the grooves of DNA.[14–16] To correctly interpret the spectroscopic features of free DAPI and in complexes with DNA and proteins, it is necessary to characterize its spectroscopic properties. In this work we combine information from linear dichroism (LD), fluorescence polarization anisotropy (FPA), circular dichroism (CD), and magnetic circular dichroism (MCD) measurements to elucidate the electronic properties of DAPI in the UV–vis region.

Materials and Methods

Chemicals. All chemicals used were of analytical grade and aqueous solutions were prepared with deionized triply filtered water (Milipore). DAPI was purchased from Serva and used without purification. Poly(vinyl alcohol) (PVA) was obtained as powder from E. I. du Pont de

(1) Kapuscinski, J.; Szer, W. *Nucleic Acids Res.* **1979**, *6*, 3519–3534.
(2) Kapuscinski, J.; Yanagi, K. *Nucleic Acids Res.* **1979**, *6*, 3535–3542.
(3) Naimski, P.; Bierzynski, A.; Fikus, M. *Anal. Biochem.* **1980**, *54*, 385–394.
(4) Kai, J.; Fanning, T. G. *Eur. J. Biochem.* **1976**, *67*, 367–371.
(5) Stepien, E.; Filutowicz, M.; Fikus, M. *Acta Biochem. Pol.* **1979**, *26*, 29–38.
(6) Mazus, B.; Falchuk, K. H.; Vallee, B. L. *Biochemistry* **1986**, *25*, 2941–2945.
(7) Williamson, D. H.; Fennel, D. J. *Methods Cell Biol.* **1975**, *12*, 335–351.
(8) Schweizer, D. *Exp. Cell Res.* **1976**, *102*, 408–409.
(9) Langlois, R. G.; Carrano, A. V.; Stay, J. W.; van Dilla, M. A. *Chromosoma* **1980**, *77*, 229–251.
(10) Coleman, A. W.; Maguire, M. J.; Coleman, J. R. *J. Histochem. Cytochem.* **1981**, *29*, 959–968.
(11) Tijssen, J. P. F.; Beekes, H. W.; van Steveninck, J. *Biochem. Biophys. Acta* **1982**, *721*, 394–398.
(12) Lee, G. M.; Thornthwaite, J. T.; Rasch, E. M. *Anal. Biochem.* **1984**, *137*, 221–226.
(13) Lin, M. S.; Alfi, O. S.; Donnell, G. N. *Can. J. Genet. Cytol.* **1976**, *18*, 545–547.
(14) Manzini, G.; Barcellona, M. L.; Avitabile, M.; Quadrofoglio, F. *Nucleic Acids Res.* **1983**, *11*, 8861–8876.
(15) Kubista, M.; Åkerman, B.; Nordén, B. *Biochemistry* **1988**, *26*, 4545–4553.
(16) Kubista, M.; Åkerman, B.; Nordén, B. *J. Phys. Chem.* **1988**, *92*, 2352–2356.

0002-7863/89/1511-7031$01.50/0

Nemours Co (Elvanol 71-30) and was hydrolyzed in NaOH and precipitated in ethanol prior to use.

Film Preparation. PVA was dissolved in water (10% w/v) under mild heating. Aliquots of 5 mL were taken, and 3 mL of aqueous DAPI solution was added, yielding a final DAPI concentration of 0–10 mM. The aliquots were gently poured on horizontal glass or Teflon plates and left to dry in a dust-free environment for about 24 h. The films were then removed with a spatula and, when desired, stretched mechanically under the air of a hair dryer (≈80 °C) by a factor of 3–5.

Linear dichroism (LD) at a given wavelength is defined as

$$\mathrm{LD}(\lambda) = A_{\parallel}(\lambda) - A_{\perp}(\lambda) \tag{1}$$

where $A_{\parallel}(\lambda)$ and $A_{\perp}(\lambda)$ are absorption spectra measured with plane-polarized light with a polarization parallel and perpendicular, respectively, to the macroscopic direction of orientation (in this case the direction of film stretch). The spectra were measured on DAPI oriented in stretched PVA films that were mounted in square holders to avoid relaxation. The holders had a small aperture to ensure that essentially the same part of the film was illuminated in all measurements.

Measurements in the UV–vis region were performed on a CARY 2300 spectrophotometer interfaced with an PC-AT IBM compatible computer. Five data points were collected per nanometer by using a spectral band width of 0.5 nm, and each spectrum was an average of five scans. Interference patterns in the spectra, due to reflections in the two parallel surfaces of the film, were diminished by using a smoothing function set at high frequency to avoid distortions of spectral features.

In the IR region the measurements were performed on a Perkin-Elmer 1800 instrument using an MCT narrow band detector for the region 4000–700 cm^{-1} and a dTGS detector down to 400 cm^{-1}. The nominal resolution was 2 cm^{-1}, and every spectrum was an average of 1000 scans.

The reduced linear dichroism was calculated from

$$\mathrm{LD}^{r}(\lambda) = \mathrm{LD}(\lambda)/A_{\mathrm{iso}}(\lambda) \tag{2}$$

where $A_{\mathrm{iso}}(\lambda)$ is the absorption of a corresponding isotropic sample. For a uniaxial orientation, such as in a polymer film,[17] A_{iso} can be calculated from the polarized component spectra:

$$A_{\mathrm{iso}}(\lambda) = \tfrac{1}{3}[A_{\parallel}(\lambda) + 2A_{\perp}(\lambda)] \tag{3}$$

The LD^{r} of a pure transition i is related to the direction of the absorbing transition moment as[18]

$$\mathrm{LD}^{r}_{i} = \frac{\epsilon_{xi}(\lambda)S_{xx} + \epsilon_{yi}(\lambda)S_{yy} + \epsilon_{zi}(\lambda)S_{zz}}{\tfrac{1}{3}[\epsilon_{xi}(\lambda) + \epsilon_{yi}(\lambda) + \epsilon_{zi}(\lambda)]} \tag{4}$$

where the S_{ii}'s are Saupe order parameters describing the orientation of the solute molecules,[17,19] and ϵ_i's are the diagonal elements of the extinction coefficient tensor. For overlapping transitions the observed LD^{r} is a weighted average of the LD^{r}_{i}'s of the contributing transitions:[18]

$$\mathrm{LD}^{r}(\lambda) = \sum_i \epsilon_i(\lambda)\mathrm{LD}^{r}_{i}/\sum_i \epsilon_i(\lambda) \tag{5}$$

Fluorescence polarization anisotropy (FPA) was measured on DAPI dissolved in an unstretched PVA film on an AMINCO SPF-500 "corrected spectra" spectrofluorimeter. The absorption was measured with polarizers set either vertically (V) or horizontally (H) in both the incoming and emerging light beams. The FPA was calculated from

$$\mathrm{FPA}(\lambda) = \frac{I_{\mathrm{VV}}(\lambda) - I_{\mathrm{VH}}(\lambda)G(\lambda)}{I_{\mathrm{VV}}(\lambda) + 2I_{\mathrm{VH}}(\lambda)G(\lambda)} \tag{6}$$

where G is the ratio $I_{\mathrm{HV}}/I_{\mathrm{HH}}$ used for instrumental correction. The first index refers to the excitation polarizer and the second to the emission polarizer. For DAPI in PVA the anisotropy at high excitation wavelengths reached the theoretical limit of 0.4, meaning that no reorientation of the DAPI molecules occurs within the fluorescence lifetime. This means that the anisotropy of a pure transition i is related to the angle (β_i) between the ith transition moment of absorption and the emission moment of the lowest energy transition ($i = 1$):[20]

$$\mathrm{FPA}_i = 0.4(3\cos^2\beta_i - 1)/2 \tag{7}$$

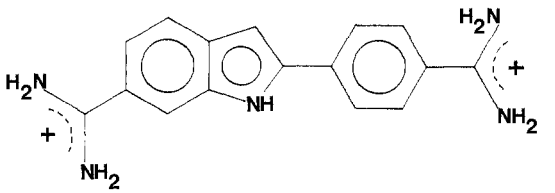

Figure 1. Molecular structure of the divalent cation 4′,6-diamidino-2-phenylindole (DAPI).

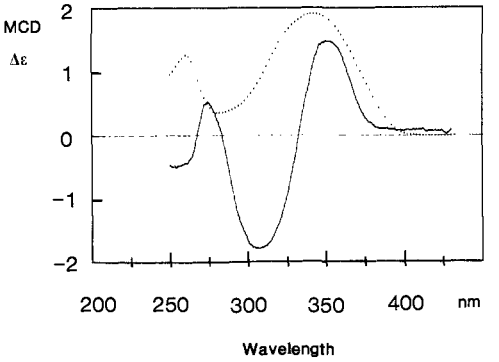

Figure 2. MCD spectrum (—) and absorption profile (···) of DAPI in aqueous solution. Cell length 2 mm, [DAPI] = 170 μM, neutral pH.

For DAPI the fluorescence quantum yield is independent of excitation wavelength (obeying the Kasha–Vavilov rules),[21] and the observed FPA is a weighted average according to

$$\mathrm{FPA}(\lambda) = \sum_i \epsilon_i(\lambda)\mathrm{FPA}_i/\sum_i \epsilon_i(\lambda) \tag{8}$$

In the PVA film the DAPI emission profile was independent of excitation wavelength and vice versa.

Circular dichroism (CD) is defined as the differential absorption of two circularly polarized beams:

$$\mathrm{CD}(\lambda) = A_{\mathrm{l}}(\lambda) - A_{\mathrm{r}}(\lambda) \tag{9}$$

where A_{l} and A_{r} are the absorption spectra measured with left and right circularly polarized light. DAPI by itself does not exhibit CD, but either bound to a chiral host or dissolved in a chiral solvent it acquires CD. The profile of the so-called induced CD is expected to be similar to the corresponding absorption band if a single transition contributes.[20] CD measurement were made on DAPI bound to DNA (calf thymus, Sigma type I) and on DAPI dissolved in *d*-tartrate at neutral pH. The measurements were made on a Jasco J-500 spectropolarimeter, which was calibrated by using the dichrometer formula.[22]

Magnetic circular dichroism (MCD) on DAPI in aqueous solution was measured on the Jasco instrument equipped with a permanent horseshoe magnet as described earlier.[23] The spectrum was recorded with both NS (north–south) and SN magnetic field orientation. The two spectra were subtracted and divided by 2 to eliminate any CD effects. The MCD of the solvent was recorded accordingly and subtracted. The gap between the magnetic poles was 2 mm, and the effective magnetic field was calibrated from the MCD signal at 510 nm of a standard 1 M $CoSO_4$ solution ($\Delta\epsilon_{\mathrm{m}} = -1.88 \times 10^{-2}\ \mathrm{M}^{-1}\ \mathrm{cm}^{-1}\ \mathrm{T}^{-1}$).[24]

The MCD signal, estimated by perturbation theory, is a sum of three terms.[17] For transitions where neither ground nor excited states are degenerate, which is the case for all transitions in DAPI because of the low molecular symmetry, only the so-called B term contributes to MCD:[17]

$$B(0f) = \sum_{k=1} \bar{\nu}_k^{-1}\langle 0|\hat{\mathbf{m}}|k\rangle\cdot\langle 0|\hat{\mu}|k\rangle\times\langle f|\hat{\mu}|0\rangle + \sum_{k\neq f} (\bar{\nu}_k - \bar{\nu}_f)^{-1}\langle k|\hat{\mathbf{m}}|f\rangle\cdot\langle 0|\hat{\mu}|k\rangle\times\langle f|\hat{\mu}|0\rangle \tag{10}$$

where $\hat{\mu}$ and $\hat{\mathbf{m}}$ are the electric and magnetic dipole operators and 0

(17) Michl, J.; Thulstrup, E. W. *Spectroscopy with Polarized Light*; VCH Publishers: New York, 1986.
(18) Nordén, B. *Appl. Spectrosc. Rev.* **1978**, *14*, 157–248.
(19) Saupe, A. *Mol. Cryst.* **1966**, *1*, 527–540.
(20) Cantor, R. C.; Schimmel, P. R. *Biophysical Chemistry*; W. H. Freeman: San Francisco, 1980; Vol. II, pp 409–480.
(21) Turro, N. J. *Modern Molecular Photochemistry*; Benjamin Cummings Publishers: California, 1978; pp 103–105.
(22) Nordén, B.; Seth, S. *Appl. Spectrosc.* **1985**, *39*, 647–655.
(23) Nordén, B.; Håkansson, B.; Danielsson, S. *Chem. Scr.* **1977**, *11*, 52–56.
(24) McCaffery, A. J.; Stephens, P. J.; Schatz, P. N. *Inorg. Chem.* **1967**, *6*, 1614–1625.

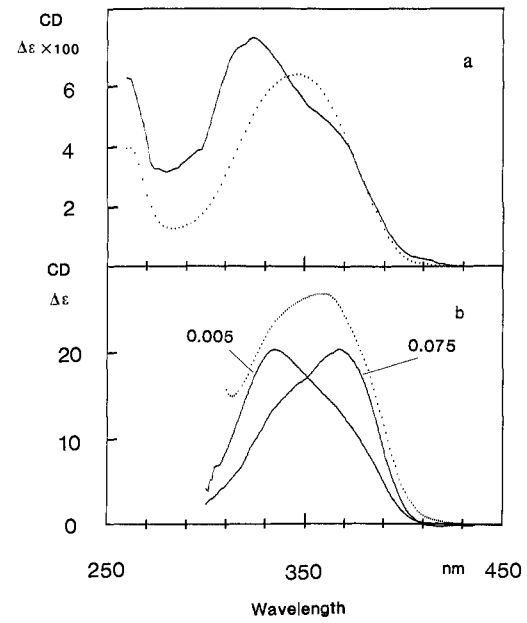

Figure 3. (a) CD spectrum (—) and absorption profile (···) of DAPI in 2 M *d*-tartrate. [DAPI] = 700 μM, neutral pH. (b) CD spectra (—) at 0.005 and 0.075 DAPI/phosphate ratio and absorption profile (···) of DAPI bound to DNA. [DNA] = 0.33 and 3.58 mM in phosphate at high and low ratio, respectively. [Na^+] = 10 mM, [EDTA] = 100 μM. All DAPI is quantitatively bound at these ratios.[15] CD spectra normalized to unit DAPI concentrations.

(ground), k, and f (final) represent wave functions in bracket notation. The sums runs over all electronic states, and $\tilde{\nu}_k$ is the energy of state k relative to the ground state in reciprocal centimeters. If vibronic interactions are small, the spectral shape of each MCD B term is expected to be similar to the corresponding absorption.[17]

Results

The divalent cation 4′,6-diamidino-2-phenylindole (DAPI) consists of a joint phenyl and indole chromophore, each with an auxochromic amidino group attached (Figure 1).

Figure 2 shows absorption and MCD spectra of DAPI in aqueous solution at neutral pH. The lowest absorption band, which gives rise to the yellow color of DAPI, is a broad, rather symmetric band with a maximum at 342 nm in aqueous solution. Such band is not observed for isolated phenyl and indole chromophores but is present in 2-phenyl substituted five-membered N-heterocyclic compounds, where it has been suggested to originate from the conjugation between the two chromophores.[25] At lower wavelengths distinct absorption peaks are observed around 260 and 224 nm. The MCD spectrum for the wavelength region corresponding to the first broad absorption band is bisignate with two lobes of essentially the same magnitude, indicating the presence of two transitions in this region. Around 275 nm an additional positive MCD peak is observed.

In Figure 3 the induced CD of DAPI dissolved in *d*-tartrate is shown. It is seen that the CD band at low energy has a completely different shape than the corresponding absorption band: a maximum is observed at 325 nm and a shoulder at about 370 nm. It has earlier been shown that DAPI acquires CD when bound to DNA and that the CD strongly depends on the molar DAPI/DNA ratio.[14,15] Figure 3b shows the CD spectra of DAPI bound to DNA at 0.005 and 0.075 DAPI/phosphate ratios. The two CD spectra are clearly different: the spectrum at high ratio is essentially a "mirror" image of the spectrum at low ratio (the shoulder in the first spectrum is a peak in the order and vice versa). When one compares the different CD profiles of DAPI above and recalls that the CD profile of a single transition is expected to be similar to the corresponding absorption profile,[20] these data clearly demonstrate that more than one transition contributes to the broad low-energy absorption band of DAPI.

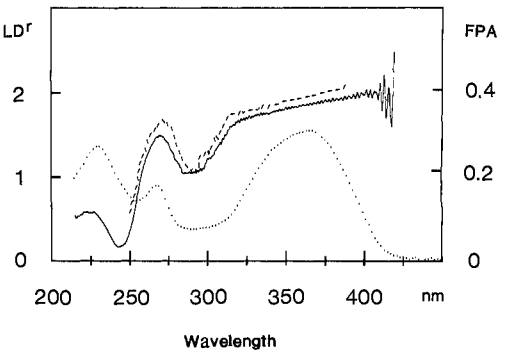

Figure 4. LD^r (—) and FPA (---) spectra and absorption profile (···) of DAPI in PVA film. For LD measurements the film was stretched by a factor of 4, yielding a final thickness of about 0.1 mm.

Figure 4 shows the isotropic absorption (A_{iso}) and LD^r spectra of DAPI in stretched poly(vinyl alcohol) (PVA) film and fluorescence polarization anisotropy (FPA) spectrum of DAPI in an isotropic PVA film. The absorption spectrum in the film is similar to the spectrum in water solution (Figures 2 and 6), indicating that electronic interaction with the PVA matrix is negligible. Both LD^r and FPA spectra display a significant wavelength dependence, showing that the effective transition moment polarization changes with wavelength. At the high wavelength edge of the FPA spectrum the theoretical limit of 0.4 is reached (cf. eq 4), indicating that no reorientation of DAPI molecules occurs during the excited-state lifetime and that the transition moment of emission is parallel to the transition moment of absorption for the first electronic transition. Both LD^r and FPA spectra have their maximum positive value at high wavelength, which decreases slightly with wavelength down to about 320 nm, after which both spectra drop to a much lower value at about 290 nm. At further lower wavelengths a local maximum in both LD^r and FPA is observed (≈270 nm), followed by a second minimum (≈244 nm). This behavior of LD^r and FPA clearly demonstrates that several transitions, with different moment polarizations, contribute to the UV–vis absorption spectrum of DAPI.

In the polarized IR spectrum of DAPI oriented in PVA film a broad range of dichroic values for the different transitions was found. Although the assignment of the different vibrational peaks is out of the scope of this study, the extreme IR dichroic values can be used to estimate the orientation of the DAPI molecule in the polymer film. For planar or rodlike molecules, a set of constant, largely negative LD^r values is expected for out-of-plane transitions. Because of the relatively large IR absorption of the PVA matrix, only three IR out-of-plane transitions of DAPI could be characterized. The LD^r for these transitions was found to be -1 ± 0.1.

Discussion

Two Overlapping Transitions That Contribute to the Low-Energy Absorption Band of DAPI. From the wavelength dependence in the region 320–450 nm in LD^r and FPA spectra of DAPI in PVA film (Figure 4) follows that the effective transition moment polarization in this region is not constant. For a pure electronic transition the transition moment polarization is independent of wavelength (cf. eq 4). Therefore, these results imply that the broad absorption band in this wavelength region is due either to a vibronic band with mixed polarization because of vibronic intensity borrowing or to two overlapping electronic transitions, each with a unique moment polarization. These two possibilities cannot be distinguished by LD and FPA measurements.

The CD profile of a single electronic transition is expected to be similar in shape to the corresponding absorption band.[20] The generally observed minor differences in shape between CD and absorption bands can usually be ascribed to vibrations that mix excited states and give rise to both negative and positive contributions to CD, whereas they give only positive contributions to

(25) Durmis, J.; Karvaš, M.; Maňásek, Z. *Coll. Czech. Chem. Commun.* **1973**, *38*, 224–242.

absorption. For the lowest absorption band of DAPI, CD bands with drastically different shapes are observed under various conditions (Figure 3). Since the extinction maximum of this band is rather large (ϵ_{344} = 23 030 M^{-1} cm^{-1}),[26] electronic transitions in this region are essentially allowed and vibronic mixing is not expected to be important. Therefore, the drastically different shapes of these CD spectra suggest that more than one electronic transition contributes to the broad low-energy absorption band of DAPI.

From eq 10 follows that if two transitions are very close in energy and have nonparallel transition moments, the MCD B term will be dominated by the mixing of the corresponding excited states:

$$B(01) = (\tilde{\nu}_2 - \tilde{\nu}_1)^{-1}\langle 2|\hat{\mathfrak{m}}|1\rangle\cdot\langle 0|\hat{\mu}|2\rangle\times\langle 1|\hat{\mu}|0\rangle$$

$$B(02) = (\tilde{\nu}_1 - \tilde{\nu}_2)^{-1}\langle 1|\hat{\mathfrak{m}}|2\rangle\cdot\langle 0|\hat{\mu}|1\rangle\times\langle 2|\hat{\mu}|0\rangle \qquad (11)$$

The MCD signals for these transitions will be equal in magnitude but have opposite signs. For the low-energy absorption band of DAPI the corresponding MCD band is bisignate (Figure 2), supporting the conclusion that this band is not due to a single electronic transition. It is not likely that more than two transitions contribute to this spectral region since the MCD spectrum changes signs only once. Further, the unstructured MCD spectrum indicates that neither of the two contributing electronic transitions has a pronounced vibrational structure.

Assignment of UV–vis Transitions. As shown above, the absorption of DAPI in the region 310–450 nm is due to two electronic transitions. Two other electronic transitions are expected to be found around 230 and 270 nm as judged from the pronounced absorption peaks at these wavelengths. In the absorption spectrum significant intensity is observed also around 290 nm, which might be due to a weak transition. At this wavelength a significant drop in both LD^r and FPA is observed. Since both LD^r and FPA spectra are weighted averages of the contributing transitions (eq 5 and 8), this drop cannot be explained by an overlap of the transition around 270 and those in the 310–450-nm region, since all these transitions have evidently a large positive LD^r as well as FPA. Therefore, we conclude that an additional transition dominates the absorption spectrum around 290 nm. In the component spectra ($A_\parallel$, $A_\perp$) the maximum of the high-energy absorption peak is found at slightly different wavelengths (results not shown), which appears as a wavelength dependence in the LD^r spectrum in this region (Figure 4). This finding indicates that the high-energy absorption peak cannot be pure and must be due to an overlap of two electronic transitions. Therefore, six electronic transitions are expected to contribute to the absorption spectrum of DAPI in the region 215–450 nm.

To determine the transition moment directions and oscillator strengths of these transitions, we must first determine their individual LD^r values and the orientation parameters that describe the molecular orientation (cf. eq 4).

For significant spectral features, such as pronounced bands, a method based on an analysis of linear combinations of the polarized absorption spectra ($A_\perp - dA_\parallel$) can be used to estimate the dichroic values for the corresponding transitions.[17] The subtraction coefficient (d_i) for which the spectral feature disappears in the linear combination is related to the dichroic value of the transition containing the feature:

$$LD^r_i = 3\frac{1 - d_i}{1 + 2d_i} \qquad (12)$$

This is illustrated in Figure 5, where, for example, the feature (peak) around 270 nm disappears for d = 0.18, which corresponds to an LD^r of 1.81. The dichroic values for the various transitions obtained this way are summarized in Table I. Although this method works reasonable well for the transitions around 220 and 270 nm, it is rather unreliable for the two transitions in the region 310–450 nm as well as for the weak transition around 290 nm, because of the absence of significant spectral features. To estimate the dichroic values for the other transitions, we have to use a different approach.

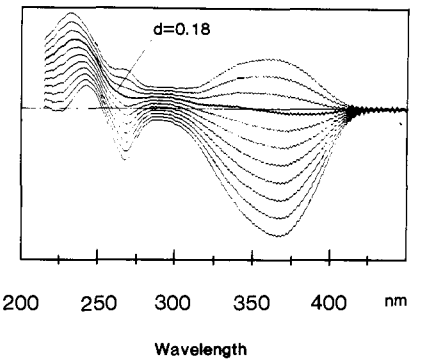

Figure 5. Linear combinations ($A_\perp - dA_\parallel$) between the two polarized absorption spectra of DAPI in PVA film. The coefficient d is varied between 0 and 0.6 in steps of 0.06. The combination for which the feature at 260 nm disappears (d = 0.18) is shown with bold line.

Table I. Parametric Description of Electronic Transitions Comprising the UV–Vis Absorption Spectrum of DAPI

λ_{max},[a] nm	half-width,[b] nm	dip str,[c] D^2	LD^r [d]	mom. pol,[e] deg
363 (380)	22 (24)	8.5	1.99 (1.96)	0–5
334 (347)	32 (32)	32.8	1.75 (1.81)	15–17
285 (290)	11 (21)	1.5	0.76 (<0.98)	≈40
260 (267)	13 (11)	10.7	1.83 (1.81)	12–19
224 (≈230)	22 (≈22)	29.9	≈0.2 (<0.19)[f]	≥50[f]
<195 (—)	≥10 (—)	>21	(<0.19)[f]	≥50[f]

[a] In aqueous solution at neutral pH. Film values given in parentheses. [b] Half-width at ϵ_{max}/e. Film values given in parentheses. [c] Dipole strength in aqueous solution estimated from $D = 9.18 \times 10^{-3}\epsilon_{max}\int\lambda^{-1}\exp(-(\lambda - \lambda_0)^2/\Delta^2)\,d\lambda\ D^2$, where λ_0 is the wavelength at peak maximum (ϵ_{max}) and Δ is the half-width.[20] The integral is calculated between $\lambda_0 \pm 100$ nm by using the $^1/_3$ Simpsons rule. ϵ_{max} is obtained by assuming ϵ_{344} = 23 030 M^{-1} cm^{-1}.[26] [d] From $3(\epsilon_\parallel - \epsilon_\perp)/(\epsilon_\parallel + 2\epsilon_\perp)$, using ϵ's from a Gaussian fit of polarized absorption spectra. LD^r is from analysis of linear combinations (Figure 5) given in parentheses. [e] Absolute angles between the transition moments and the orientation direction of DAPI in PVA film, which is within 10° to the phenyl–indole bond. [f] Refers to the transition dominating the absorption spectrum in film at 240 nm.

Since all spectral features, such as peaks, shoulders, etc., in the absorption spectrum of DAPI have been ascribed to separate electronic transitions, it is reasonable to assume that each electronic transition gives rise to a relatively unstructured contribution. For the two overlapping transitions in the 310–450-nm region this assumption is further supported by the totally unstructured MCD spectrum (Figure 2) and the lack of additional spectral features in CD (Figure 3). If spectral broadening is dominated by inhomogeneous broadening due to solvent effects, it is reasonable to assume Gaussian shapes for all electronic transitions.[27]

The two polarized absorption spectra of DAPI in PVA film were fitted by assuming Gaussian shapes. Six Gaussians were used in the fit, which was made globally to ensure the same energy maximum and half-width for each electronic transition in both component spectra. Fits to the separate components or to LD^r and A_{iso} revealed no significant differences. The goodness of the fit, judged from calculated sum-of-squares values, was found to be very sensitive to the parameters for the four low-energy Gaussians, and these are therefore believed to be highly accurate. For the two high-energy transitions decent fits could be obtained with a rather broad range of parameters, and these are therefore less reliable. The parameters obtained from the fit are listed in

(26) Masotti, L.; Cavatorta, P.; Avitabile, M.; Barcellona, M. L.; von Berger, J.; Ragusa, N. *Ital. J. Biochem.* **1982**, *31*, 90–99.

(27) Barker, B. E.; Fox, M. F. *Chem. Soc. Rev.* **1980**, *9*, 143–184.

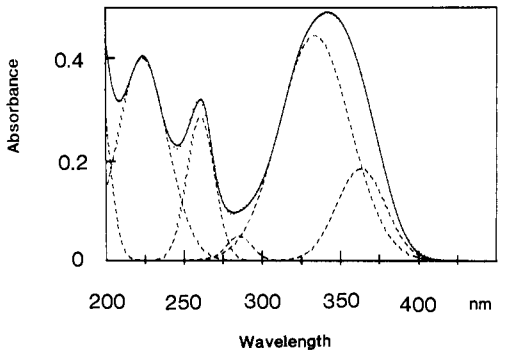

Figure 6. Measured (—) and fitted (···) absorption spectra of DAPI in aqueous solution resolved into Gaussian components (---). [DAPI] = 18 μM, neutral pH.

Table I, and a corresponding fit to the absorption spectrum in water is shown in Figure 6.

Determination of Transition Moment Polarizations. The dichroic values for the electronic transitions obtained from the fit are related to the corresponding transition moment directions according to eq 4. To solve this equation, we first have to estimate the order parameters (S_{xx}, S_{yy}, and S_{zz}), i.e., the orientation of the DAPI molecules in the PVA film.

As seen in Figure 4, the wavelength dependence in the FPA spectrum is within experimental error the same as in the LD^r spectrum. From this follows that the dichroic values (LD^r_i in eq 5) must equal the anisotropies (FPA_i in eq 8) for all transitions. This is the case when $S_{xx} = S_{yy}$, which corresponds to a rodlike orientation. In such situation eq 4 simplifies to[18]

$$LD^r_i = \frac{3\cos^2\theta_i - 1}{2}(3S_{zz}) \qquad (13)$$

where θ_i is the angle between the ith transition moment and the molecular orientation axis. Further, the θ_i angles must equal the β_i angles in eq 7, which corresponds to a situation where the transition moment of emission coincides with the molecular orientation axis.

An essentially rodlike orientation is indeed expected from the elongated shape of DAPI and from the fact that the molecule may be somewhat twisted. By comparing eq 7 with eq 13, it is found that the scale factor between the FPA and LD^r spectrum corresponds to $3S_{zz}/0.4$. The scale factor between the two spectra is about 4.9 (shown in Figure 4 with a scale factor of 5 for clarity), which yields $S_{zz} = 0.66$. The highest possible dichroic value is then 1.98 ($\theta = 0$ in eq 13). The LD^r spectrum reaches a value of about 2 at the low-energy edge, which indicates that the transition moment of absorption for the lowest energy transition is parallel to the molecular orientation axis. Since this moment is also parallel to the transition moment of emission, as judged from the limiting FPA value of 0.4, all θ_i angles are indeed expected to equal the β_i angles. A rodlike orientation is also supported from the dichroic values of the IR out-of-plane transitions. For such orientation the dichroic value of a transition polarized perpendicularly to the unique axis is expected to be half the negative value of the dichroic value of a transition polarized along the unique axis ($\theta_i = 0°$ and 90° in eq 13). The LD^r of the out-of-plane IR transitions was found to be -1 ± 0.1, which agrees well with the LD^r of 2 observed for the low-energy UV–vis transition.

From the known molecular orientation we calculate the transition moment angles using eq 13 (Table I). These angles relate the transition moment directions to the so far unknown orientation axis of DAPI which coincides with the transition moment direction of the first electronic transition. We shall, however, argue that it is likely that this axis is along the bond joining the phenyl and indole chromophores. The elongate molecular shape of DAPI suggest an essentially long-axis orientation. Further, the low-energy absorption band is not present in the isolated indole and phenyl chromophores but appears in 2-phenylindole.[25] This suggests that the new transitions comprising this band involve both chromophores, and therefore the corresponding moments should be polarized along a vector connecting them. The moment direction of the first electronic transition is also found to be close to the phenyl–indole bond (within 10°) by semiempirical calculations (not shown).

Conclusions

From our results we conclude that the broad, low-energy absorption band at near-UV of 4′,6-diamidino-2-phenylindole is due to two different electronic transitions. The transition moment directions of both transitions is essentially parallel to the phenyl–indole bond. We also characterize four additional electronic transitions in the UV–vis absorption spectrum of DAPI.

Acknowledgment. This project is supported by the Natural Swedish Research Council and the Swedish Board for Technical Development.